An investigation of the shoaling of large amplitude internal waves using computational fluid dynamics

R P Hornby[1] & R J Small[2]
[1]*Defence Science and Technology Laboratory (Dstl), Winfrith, UK.*
[2]*International Pacific Research Centre, Hawaii.*

Abstract

The transformation of internal waves in shallow water is important for studies of energy dissipation and for enhanced mixing of nutrients and pollutants in the ocean. The wave transformations are also important because they affect the propagation of sound in the upper surface layers of the ocean and the flows induced by the waves may affect moored oil platforms and submersibles.

In this paper attention is focussed on the behaviour of a typical large amplitude internal wave passing into shallow water. A Computational Fluid Dynamics (CFD) code is used to solve the full, two-dimensional time dependent conservation equations for the fluid. Turbulence is modelled using a two equation turbulence model with account taken of the effects of stratification on turbulence.

The CFD simulations predict the wave transformations occurring as the primary wave propagates on-shelf and the velocity distributions, turbulence production and fluid transport induced by passage of the waves.

1 Introduction

Large amplitude internal waves (which may evolve into isolated waves of fixed form called solitary waves) are commonly produced at continental shelf breaks (and other local topographic features) by tidal forcing. These waves have amplitudes of order tens of metres and horizontal particle velocities of order

tens of centimetres per second, and they therefore significantly affect the local stratification and current shear.

Shoaling of these waves leads to wave steepening which ultimately results in wave breaking [1]. The breaking process redistributes tidal energy into higher frequency waves and turbulence; this results in enhanced mixing, which spreads nutrients and sediments into the water column. An understanding of the mixing produced by these events is important in the mixing formulations used by larger scale models. The large localised perturbations to the ocean structure caused by these phenomena also affect the propagation of sound in the upper surface layers of the ocean [2]. The propagation of these waves and the way in which they interact with bathymetry are therefore significant aspects to consider when making an assessment of the performance of underwater acoustic sensors. The burst of current associated with passage of these waves can induce sufficient strain on moored oil platforms to affect the platform safety [3]. Measures have to be in place to alleviate such strains which means that methods are required to compute the strains and predict the arrival time of the waves. The increased variability of current and density gradient may also be expected to have an effect on the motion of submersibles and safety of divers.

The equations governing the propagation of large amplitude internal waves are inherently non-linear and the non-linear effects are accentuated by shoaling. The latter has been studied in terms of weakly non-linear theory [4-6]. For many typical deep seasonal oceanic scenarios of a thin upper layer over a deep lower layer, the propagating internal wave is one of depression producing a downward displacement of the pycnocline. In shallow water where the upper layer may be thicker than the lower layer, a wave of elevation is propagated. In a shoaling process, both situations may arise. According to weakly non-linear theory, as a solitary wave approaches shallow water and the transition zone from wave of depression to wave of elevation, the forward face becomes less steep and aligns with the bathymetry while the back face steepens and then starts to form an undular bore. The undulations then become distinct solitary waves of elevation [6].

The objective of the current work is to show that commercially available CFD codes, which solve the full non-linear equations, can be used to predict the detail of the shoaling processes of large amplitude internal waves (a common occurrence in summer in stratified coastal waters when internal waves propagate towards the coast). Good results may be obtained from the weakly non-linear theory when the modelling assumptions are satisfied but in complex interactions this may be difficult to assess and the accuracy of the results is then questionable.

The advantages of using CFD lie in its ease of use, general applicability and availability of a wide variety of modelling techniques. Hornby and Small [7] describe some exploratory computations of internal wave propagation using CFD and comparisons with weakly non-linear theory. However, the considerations of accuracy were limited to large amplitude internal waves propagating in water of uniform depth. Here, attention is focussed on the spatial

and temporal grid requirements to compute different aspects of the internal wave shoaling process.

2 Governing equations

The problem is studied numerically using the PHOENICS CFD code which solves the non-linear equations for conservation of mass, momentum, energy, turbulent kinetic energy, turbulent energy dissipation rate and tracer concentration on a fine grid. These equations can be written in general transport form in Cartesian (x_1, x_2, x_3) coordinates as,

$$\frac{\partial(\rho\phi)}{\partial t}+\frac{\partial(\rho u_j\phi)}{\partial x_j}=\frac{\partial(\Gamma_\phi\frac{\partial\phi}{\partial x_j})}{\partial x_j}+S_\phi \qquad (1)$$

where ϕ is 1 for mass conservation, u_1, u_2 or u_3 for momentum conservation, ρ for density transport, k for turbulent kinetic energy transport, ε for turbulent energy dissipation rate transport and c for tracer concentration transport. Γ_ϕ and S_ϕ are the exchange coefficient and source term for ϕ. For the momentum equations the pressure gradient term and (full) buoyancy source term are included in S_ϕ. Coriolis terms are not included since the Rossby number is large at mid-latitudes for velocity and length scales associated with large amplitude internal waves.

These equations are solved for generalised stratification and arbitrary bathymetry in 2-D Cartesian coordinates with the x coordinate taken as range and the y coordinate as vertical distance. A 2-D representation is considered satisfactory as the radius of curvature of the wavefronts is large in comparison to the range distance over which significant shoaling effects take place. A 3rd order upwind scheme [8] is used for the spatial discretisation. Time discretisation is first order (high order temporal schemes are not generally available in PHOENICS). A standard k, ε turbulence closure [9] with a buoyancy source term in the k and ε equations dependent on the density gradient (to model the effects of stratification on turbulence, [10]) is used. The constant $C_{3\varepsilon}$ in the ε equation is set equal to 0.2 as recommended by Rodi [11] for stable stratification. The bathymetry is modelled using cell porosity.

Initial waveforms in the domain may be prescribed from analytical approximations or from measured waveforms in the ocean. The lateral boundaries have a prescribed hydrostatic pressure determined from the stratification and may act as inflow or outflow boundaries. The ocean surface is represented as a rigid lid to good approximation since the surface elevations induced by internal waves are small compared to the internal wave amplitude. In addition, it is treated as a free-slip boundary. The bottom surface stress is included as a source for the horizontal momentum equation with a value calculated using the flow velocity at 1m from the sea bottom and a drag coefficient of 0.0025 (sandy/gravel bottom, [12]). k, ε values at the grid node

adjacent to the sea bottom are calculated from expressions assuming equality of production and dissipation of turbulence (the equilibrium assumption, [13]). Field values of k, ε are initialised at t=0 to low background values of 10^{-6} (m^2/s^2) and 10^{-9} (m^2/s^3 or W/kg) respectively.

3 Results and discussion

Results are presented for the shoaling of a large 25m amplitude internal wave travelling towards the coast from water of depth 141m to water of depth 70m. The wave profile and associated horizontal velocity information are taken from measurements off the Malin shelf (North West coast of Scotland) in the summer of 1995 as part of the Shelf Edge Study Acoustic Measurement Experiment (SESAME) [14]. One of the sponsors of this study was the UK Ministry of Defence (MoD) of which the Defence Science and Technology Laboratory (Dstl) now forms part. This particular case was considered in order to assess the capabilities of the CFD code for a complicated situation involving wave breaking and then the possible evolution of waves of elevation. SESAME has measurements relating to internal wave shoaling in deeper water (from 400m to 140m where the changes in wave shape are less dramatic); hence it is planned to compare this data with CFD results at a later date.

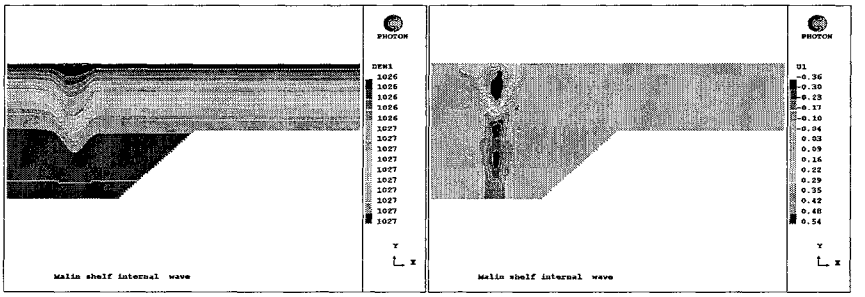

Figure 1. Malin shelf internal wave. Density (kg/m^3) field (left) and horizontal velocity (m/s) field (right) at t=0s. Slope gradient=0.05.

The water depth is 141m at the point of measurement of the wave profile. Unless specified otherwise, all vertical distance will be with reference to this maximum depth. The water column is continuously stratified with a density of 1027.28 kg/m^3 near the bottom and a density of 1025.83 kg/m^3 near the surface. Initial guidance on the spatial and temporal grid resolution has come from earlier work [7] and exploratory shoaling calculations, indicating that a cell size in the x (horizontal) direction of 10m and a cell size in the y (vertical) direction of 1m to 2m should give adequate spatial resolution. These preliminary calculations have shown that there is more uncertainty about the choice of time step particularly if detail relating to wave breaking is required. Consequently, the time step is varied between 1.25s and 10s. The horizontal extent of the

domain is 6500m (see Fig. 1), with the slope starting 2031m and terminating 3441m from the left boundary. The shelf slope gradient used is 0.05 so that the wave propagates from water at 141m deep to water at 70m deep over a distance of approximately 1400m.

A spatial grid with dx=10m and dy=2m and time step of 5s is used unless stated otherwise. All dt=5s and dt=10s runs were completed in one without restarts. The dt=2.5s results were obtained from a restart of the dt=10s run at t=4000s. The dt=1.25s results were advanced from results at t=6000s obtained from a restart of a dt=10s run to 4000s followed by a dt=2.5s run to 6000s. This was done to reduce the computing resource required for the smaller time step runs. Care was taken to ensure that as far as possible temporal convergence had been achieved at each restart.

Figure 1 shows the density and horizontal velocity distribution in the initial wave form (which is approximately 25m in amplitude). The densities were obtained using temperature and salinity measurements and the horizontal velocities (which range between -0.36m/s and 0.54m/s) from an Acoustic Doppler Current Profiler (ADCP). These initial fields are easily accommodated by the CFD code and give rise, subsequently, to a complicated, evolving flow field shown in Fig. 2. In particular, the density contours downstream of the wave exhibit a small scale variability typical of stratified ocean environments.

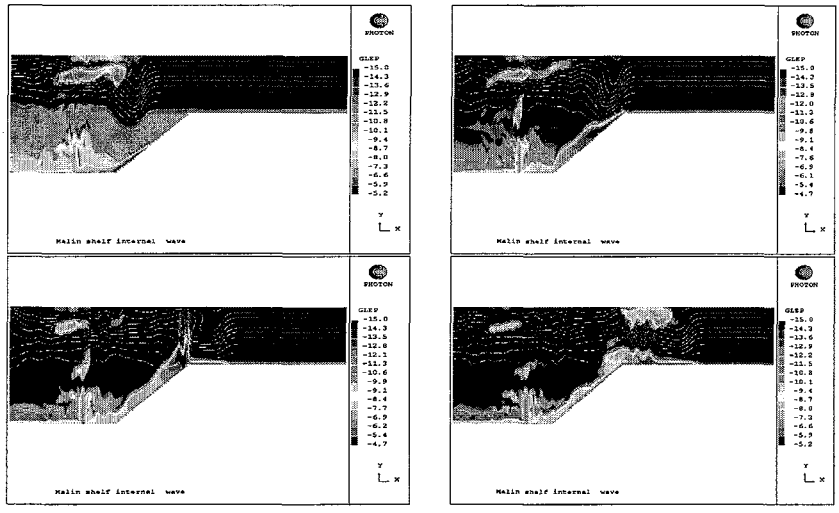

Figure 2. Malin shelf internal wave propagation showing $\log_{10}\ \varepsilon$ (m^2/s^3) with superimposed density contours; dt=5s, dy=2m, dx=10m, slope gradient=0.05. (Top left) t=2000s, (top right) t=4000s, (bottom left) t=6000s, (bottom right) t=8000s.

Figure 2 gives results at t=2000s, 4000s, 6000s and 8000s for the turbulence dissipation rate and wave shape (superimposed density contours). Note that the scales used for the turbulence dissipation rate are slightly different for each time

frame. While the main internal wave propagates towards the slope, residual fields are left at the initial wave position and persist for the duration of the simulation. This persistence is probably the result of the initial small scale activity 'deposited' by the input wave and shear from waves reflected from the left hand boundary and (later) shelf slope.

The main locations of turbulence dissipation as the wave propagates up slope are on the sea bed and there appears to be little generation of turbulence within the wave itself until the shelf edge is reached (t>6000s). In reality additional shear in the ocean environment may combine with that generated by passage of the waves to enhance turbulence production. At the shelf edge, progressive steepening and breakup of the rear face of the wave produce significant bottom and near surface turbulence. The primary wave is seen to become narrower (wavelength reduces) as it propagates up the slope but much broader as it propagates on shelf. Figure 3 shows the predictions of profiles for turbulent dissipation rate with distance from the bottom after 8000s for time steps of 10s, 5s, 2.5s and 1.25s. The profiles are taken at 4245m from the left hand boundary which corresponds to the region of near surface, on shelf turbulence production shown in Fig. 2. It can be seen that the 10s time step produces values of the near bed turbulent dissipation very similar to those obtained with shorter time steps but fails to produce the near surface turbulence. This is because the 10s time step does not adequately predict the breakup of the primary wave into smaller scale waves. The shear from these smaller scale waves appears to be responsible for the turbulence generation.

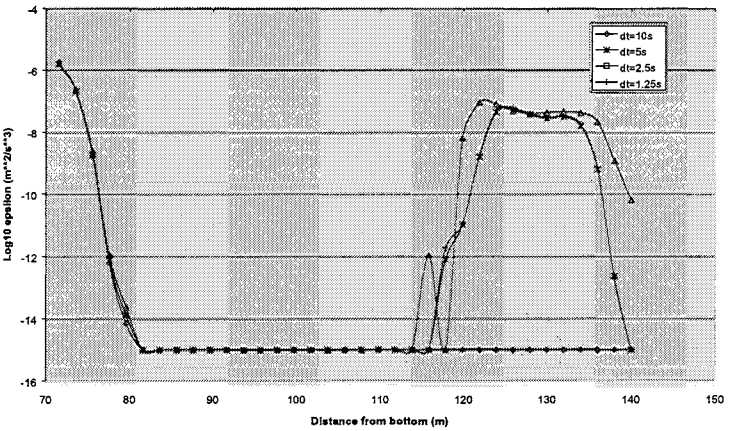

Figure 3. Malin shelf internal wave propagation showing profile of $\log_{10}\varepsilon$ (m^2/s^3) with distance (m) from bottom at x=2214m from slope start (wave on shelf); t=8000s, dy=2m, dx=10m, slope gradient=0.05.

The effect of time step on the prediction of the wave mean density profile after breaking are shown in Fig. 4 for time steps of 10s, 5s, 2.5s and 1.25s. It

can be seen that good temporal convergence of results is achieved for the primary wave shape but that significant differences between the 10s time step and 1.25s time step results are apparent for the prediction of the smaller scale waves appearing on the rear face of the primary wave. A time step of 5s is required to give reasonable resolution of these smaller scale waves and the consequent near surface turbulence generation shown in Fig. 3.

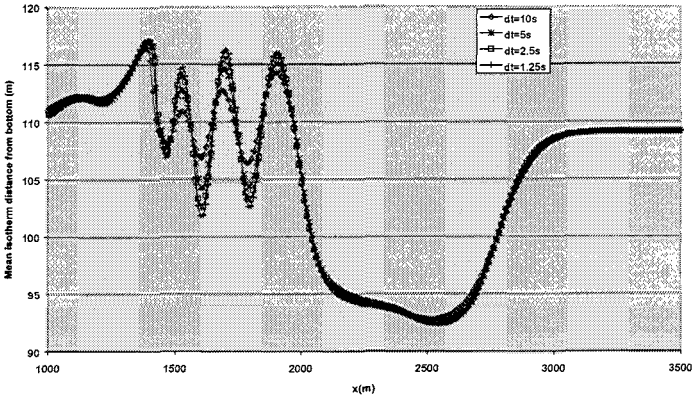

Figure 4. Distance from bottom (m) of position of mean density in wave against distance (m) from slope start at t=8000s for dy=2m, dx=10m, slope gradient=0.05 (wave on shelf). View centred around leading wave profile. x=0 marks start of slope.

The velocity distribution induced by these waves is important both for pollutant and nutrient transport and for transient forcing on moored structures. Figures 5 and 6 show the variation with range of the horizontal and vertical flow velocities at t=8000s (with the primary wave now travelling on-shelf). Figure 5 shows the horizontal velocity variation at 1m and 70m depth. Maximum horizontal velocities of 0.3m/s are associated with the primary wave. Figure 6 shows the variation of the vertical velocity component at 35m depth (mid on-shelf depth). Vertical velocities of ~0.06m/s are associated with the tail of the primary wave and the smaller scale waves resulting from breakup. Figure 5 indicates that the tail waves are probably early manifestations of waves of elevation since the horizontal velocities near the surface and at depth are of opposite sign to those in the primary wave of depression. This accords with theoretical expectations and observations and calculations by Liu [6] (note that the on-shelf stratification is not uniform with depth).

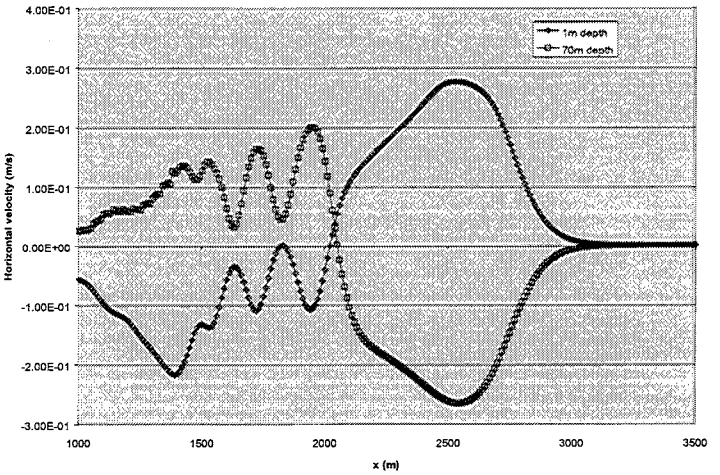

Figure 5. Malin shelf internal wave propagation; dt=5s, dy=2m, dx=10m, slope gradient=0.05. Horizontal velocity component (m/s) at 1m and 70m depth at t=8000s (wave on shelf) against distance (m) from slope start. x=0 marks start of slope.

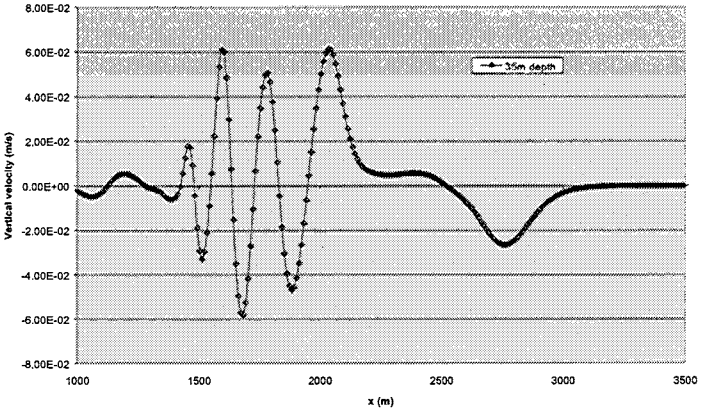

Figure 6. Malin shelf internal wave propagation; dt=5s, dy=2m, dx=10m, slope gradient=0.05. Vertical velocity component (m/s) at t=8000s (wave on shelf) at 35m depth against distance (m) from slope start. x=0 marks start of slope.

Finally Fig. 7 shows the effect of the wave passage on three continuous, line sources of tracer (at a concentration of unity) placed near the initial position of the wave, near the shelf edge and on shelf. The distortion of these concentration profiles from passage of a single wave is substantial. The main mechanism

appears to be by advective transport. In particular significant on and off shelf transport of pollutant or nutrient would be accomplished by passage of these waves.

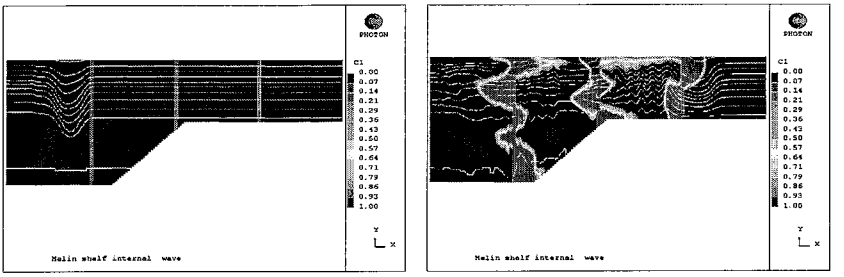

Figure 7. Malin shelf internal wave propagation; dt=5s, dy=2m, dx=10m, slope gradient=0.05. (Left) continuous tracer concentration sources with superimposed density contours at t=0s. (Right) tracer concentration sources with superimposed density contours at t=10000s.

4 Conclusions

This work constitutes part of an ongoing assessment of the capability of CFD to represent the ocean structure associated with the propagation and interaction of large amplitude internal waves. Results from a single shoaling event modelled with the PHOENICS CFD code are encouraging and have produced initial guidelines on the spatial and temporal resolution required in order to predict various aspects of the wave development. The primary wave evolution can be described with a relatively coarse spatial and temporal discretisation but the prediction of the primary wave breakup and subsequent turbulent mixing requires much finer resolution.

Further work is required to examine the characteristics of large amplitude, shoaling internal waves taking into consideration variation of wave amplitude, stratification and slope gradient. Results from the calculations need to be compared quantitatively with experiment and qualitatively with field data (the latter proviso reflects the difficulty in precisely defining the ocean environment).

The results from such simulations will enhance understanding of the environmental structure and flow distribution associated with passage of these waves and the effects that these changes have on the propagation of sound, the transport of nutrients, sediments and pollutants and the stability of moored platforms.

Acknowledgments

Thanks are given to Dstl for funding this research work and to the School of Ocean Sciences at the University of Wales (Bangor) for supply of the initial density and velocity fields for this study.

References

[1] Haury, L. R., Briscoe, M. G., & Orr, M., Tidally generated internal wave packets in Massachusetts bay. *Nature,* **278**, pp. 312-317, 1979.

[2] Prior, M. K., *Low frequency sound propagation in sea surface mixed layers and in the presence of internal waves*, Ph D Thesis , Institute of Sound and Vibration Research, University of Southampton, 1996.

[3] Bullock, J. D., & Corley, C. B., Exploration drilling in very deep water. *10th World Petroleum Congress, Bucharest,* 1979.

[4] Helfrich, K. R., & Melville, W, K., 1986, On long nonlinear internal waves over slope-shelf topography. *Journal of Fluid Mechanics,* **167**, pp. 285-308, 1986.

[5] Grimshaw, R., Pelinovsky, E., & Talipova, T., Solitary wave transformation in a medium with sign-variable quadratic non-linearity and cubic non-linearity. *Physica D*, **132**, pp. 40-62, 1999.

[6] Liu, A. K., Chang, Y. S., Hsu, M. K., & Liang, N. K., Evolution of nonlinear internal waves in the East and South China Sea. *Journal of Geophysical Research*, **103, C4**, pp. 7995-8008, 1998.

[7] Hornby, R. P., & Small, R. J., PHOENICS predictions of large amplitude internal waves in the ocean. *PHOENICS Journal*, **13**, pp. 243-258, 2000.

[8] Koren, B., *Numerical methods for advection-diffusion problems*, Vreugdenhil, C. B., & Koren, B., (eds)., Vieweg, pp. 117-138, 1993.

[9] Launder, B. E., & Spalding, D. B., The numerical computation of turbulent flows. *Computer Methods in Applied Mechanics and Engineering,* **3**, pp. 269-289, 1974.

[10] Rodi, W., *Turbulence models and their application in hydraulics*, report, International Association for Hydraulic Research, Delft, Netherlands, 1980.

[11] Rodi, W., Examples of calculation methods for flow and mixing in stratified fluids. *Journal of Geophysical Research*, **92**, pp. 5305-5328, 1987.

[12] Heathershaw, A. D., Sediment transport in the sea, on beaches and in rivers: part 1-fundamental principles. *Journal of Naval Science*, **14, 3**, 1988.

[13] Luyten, P. J., Deleersnijder, E., Ozer, J., & Ruddick, K. G., Presentation of a family of turbulence closure models for stratified shallow water flows and preliminary application to the Rhine outflow region. *Continental Shelf Research*, **16, 1**, pp. 101-130, 1996.

[14] Small, J., Sawyer, T. C., & Scott, J. C., The evolution of an internal bore at the Malin shelf-edge. *Annales Geophysicae*, **17**, pp. 547-565,1999.